



ORIGINAL PAPER

AN INVESTIGATION ON THE INFLUENCES OF INITIAL CONFINING PRESSURE ON COAL MECHANICAL PROPERTIES AND ENERGY EVOLUTION LAW

Hongjun GUO^{1,3,5)}, Zhongguang SUN²⁾, Xiaodong LI³⁾, Ming JI⁴⁾ *and Haizhu LI⁶⁾¹⁾ Jiangsu Vocational Institute of Architectural Technology, Xuzhou, 221116, China²⁾ China Coal Technology and Engineering Group Chongqing Research Institute, Chongqing, 400039, China³⁾ Xinjiang Career Technical College, Yili, 833200, China⁴⁾ Key Laboratory of Deep Coal Resource Mining, Ministry of Education of China, School of Mines, China University of Mining & Technology, Xuzhou, 221116, China⁵⁾ State Key Laboratory of Intelligent Construction and Healthy Operation and Maintenance of Deep Underground Engineering, China University of Mining & Technology, Xuzhou, 221116, China⁶⁾ School of Energy Industry, Shanxi College of Technology, Shuozhou, 036000, China*Corresponding author's e-mail: jjiming@cumt.edu.cn

ARTICLE INFO

Article history:

Received 15 December 2024

Accepted 27 January 2025

Available online 3 February 2025

Keywords:

Coal body

Unloading confining pressure and loading

Axial pressure

Initial confining pressure

Mechanical properties

Energy characteristics

Excavation unloading

ABSTRACT

Despite that new energy sources have been developing for years, coal still serves as a key resource in the energy structure in China, resulting in the deep mining as one of preferred method. In order to further explore the causes of frequent occurrence of dynamic disasters during the deep mining, the stress path of unloading confining pressure and axial pressure is designed based on the stress adjustment characteristics of the surrounding rock in the excavation roadway. The mechanical properties and energy evolution law of coal body under different initial confining pressures are studied through experiments. With the increase of initial confining pressure, the mechanical parameters of the coal body at the failure point reveals that the peak strength, confining pressure and axial strain increase nonlinearly, while the evolution law of the lateral strain and volumetric strain is not obvious. In addition, the failure mode develops into the brittle failure. In terms of the energy, the original rock energy storage, each energy (U_1 , U_3 , U , w_e , and w_d) and elastic strain energy conversion rate increase nonlinearly, indicating that high initial confining pressure (large burial depth) significantly aggravates the risk and strength of coal dynamic failure. According to the experiments, the combined pressure relief measures should be taken in the actual production process to release energy and lower the risks of failures, contributing to a safe and efficient production. It is expected that the research results can provide some insights to the deep resource development and dynamic disaster prevention and control

1. INTRODUCTION

With the gradual depletion of coal resources globally, the deep mining become widely adopted in the coal mining industry (Xie et al., 2015). At present, most of mines in central and eastern China have entered the stage of the deep mining (Kang et al., 2018). According to some preliminary statistics, by the end of 2020, the number of coal mines in China was about 4700, with more than 50 coal mines featured with a mining depth exceeding 1000 m (Huang et al., 2020). Under the influence of the complex stress environment of “three highs and one disturbance” and significant time effects, the organizational structure, basic behavior and engineering response of deep coal and rock mass have undergone some fundamental changes, resulting in many difficulties and challenges (Xie, 2019; He, 2021; Cui et al., 2021). Cui et al. (2021) believed that mining disturbance was the fundamental cause of deformation, impact and instability of deep coal and rock mass. Yuan (2021) proposed that the non-linear and non-uniformity mechanical and physical properties of deep mining coal and rock mass induced

many disasters such as the coal and gas outburst and rockburst. Zhao et al. (2021) indicated that the increase of the mining depth contributed to the hard brittle characteristics of coal and rock mass, and aggravated the probability and intensity of dynamic disasters such as rockburst (Chen et al., 2019).

For the mining industry or other large-scale underground projects such as diversion tunnels, traffic tunnels, energy storage, nuclear waste treatment, and important military and national defense facilities, a series of safety problems that are different from the deformation and failure of shallow coal and rock mass tend to take place with the increase of burial depth, especially in dynamic disasters (Zhao, 2021). In recent years, scholars in China and abroad have conducted substantial researches on the engineering characteristics of deep disturbed coal and rock mass (Guo et al., 2021, 2022a, 2022b). Based on the step loading creep test of deep soft rock, Zhou et al. (2022) established a ternary nonlinear damage hardening creep model, which can accurately determine the long-term

strength of deep soft rock. Wu et al. (2022) obtained Griffith envelope by a series of coal and rock experiments, and then explained the influences of the deep in-situ stress on surrounding rock deformation and failure. Through the mining simulation experiment Yang et al. (2020) found out that the mining layout and burial depth have a significant impact on the micro-cracks, structural evolution and stress state of coal and rock mass. Xie et al. (2019) conducted a series of coal-rock mechanics experiment and suggested that the buried depth increases the strength and range of engineering disturbance, resulting in greater difficulties in controlling the stability of roadway surrounding rock. Zhang et al. (2022) studied the response characteristics of buried depth and lateral pressure coefficient to the principal stress difference, energy and rockburst tendency of surrounding rock during the disturbance of deep engineering excavation by 3DEC numerical simulation software. Combined with the rockburst tendency laboratory test and uniaxial compression acoustic emission test of limestone with different buried depths, Wang et al. (2022) established a damage model characterized with the cumulative energy of acoustic emission. Zeng et al. (2021) established a rockburst precursor information model, which indicated that the rockburst tendency increases gradually with the increase of buried depth gradient. In addition, when the buried depth exceeds 1000 m, the limestone develops a strong rock burst tendency. Using the true triaxial rockburst experimental system, Yan et al. (2022) carried out the rockburst physical simulation experiments of granite under different burial depths of 500-1100 m, and identified that the rockburst is featured with the time delay and various stages.

The achievements made in rock mechanics of deep engineering provides important guidance for the layout design. However, the surrounding rock stability control, the disaster prevention and the safety issues are still the main factors affecting the high yield and high efficiency in the face of complex and changeable stress environment and high-strength construction requirements (Zhao, 2021). In this study, the stress adjustment process of surrounding rock in deep mine roadway excavation is thoroughly researched, along with the mechanical characteristics and energy evolution law of coal body under different initial confining pressures (i.e., buried depth) through the experiments of unloading confining pressure and loading axial pressure. It is expected that this study can provide some insights for the stability control of the surrounding rock in the deep mining roadway and the prevention and control of related dynamic disasters, contributing to the development of the safe and efficient practices in the deep engineering.

2. EXPERIMENTAL DESCRIPTIONS

2.1. EXPERIMENT PREPARATION

The coal samples were selected from #8 coal seam in the third mining area of a mine located in Xianyang mining area with an average thickness of 8.05 m, a dip angle of 4°, a density of 1.4 g/cm³, a uniaxial compressive strength of 22.3 MPa, and a maximum buried depth of nearly 800 m. According to the international rock mechanics experiment regulations, coal samples were processed into the cylinder standard specimens in the dimension of $\Phi 50 \text{ mm} \times L100 \text{ mm}$, as shown in Figure 1. The related experiments were completed by taking advantage of MTS815.02 rock mechanics testing system of China University of Mining and Technology (Fig. 2).



Fig. 1 Coal specimen.



Fig. 2 The 815.02 rock mechanics testing system.

2.2. EXPERIMENTAL SCHEME

Considering that the mining depth of most production mines is distributed in 400-1000 m, the initial confining pressure was set to 10 MPa, 15 MPa, 20 MPa and 25 MPa in the experiment to simulate the original rock stress environment being in the hydrostatic pressure state under different buried depths, with the stress adjustment of surrounding rock in roadway excavation following the stress path of

Table 1 Experiment results.

Number	Initial confining pressures σ_{30} / MPa	Lateral strain $\varepsilon_3 / 10^{-3}$	Volume strain $\varepsilon_v / 10^{-3}$	Confining pressure σ_3 / MPa	Axial strain $\varepsilon_1 / 10^{-3}$	Failure strength σ_c / MPa	Average failure strength $\bar{\sigma}_c$ / MPa
1	10	-4.177	-4.560	0.755	3.794	28.954	28.871
2	10	-4.628	-5.820	0.611	3.436	29.723	
3	10	-3.261	-2.920	0.883	3.601	27.937	
4	15	-6.806	-7.777	1.155	5.834	42.457	42.013
5	15	-7.438	-8.966	1.934	5.911	42.076	
6	15	-5.270	-6.004	1.956	4.537	41.506	
7	20	-6.458	-6.549	4.155	6.367	52.851	53.159
8	20	-4.830	-3.769	3.358	5.892	54.071	
9	20	-3.398	-1.507	4.765	5.289	52.554	
10	25	-4.938	-4.776	11.503	5.101	53.043	58.465
11	25	-5.684	-4.743	4.709	6.626	65.747	
12	25	-6.203	-5.581	9.501	6.824	56.604	

unloading confining pressure and loading axial pressure (as shown in Fig. 3). The detailed experiment process is presented below.

1. Stress control mode: in order to reduce or avoid the influence of excessive stress in one direction causing serious damage or premature failure on the specimen, follow the form of $\sigma_2=\sigma_3=5 \rightarrow \sigma_1=5 \rightarrow \sigma_2=\sigma_3=10 \rightarrow \sigma_1=10$ MPa..., and alternately increase confining pressure and axial pressure to the predetermined value 10 MPa (15 MPa, 20 MPa, and 25 MPa) at the loading rate of $v_3=v_1=0.05$ MPa/s.
2. Stress control mode: for the stress path of conventional triaxial compression, increase axial pressure σ_1 at the loading rate of $v_1=0.1$ MPa/s until the sample fails; for the stress path of unloading confining pressure and loading axial pressure, simultaneously, reduce confining pressure $\sigma_2(\sigma_3)$ at the unloading rate of $v_3=0.05$ MPa/s, and increase axial pressure σ_1 at the loading rate of $v_1=0.1$ MPa/s until the sample fails.

3. ANALYSIS AND DISCUSSIONS

The deformation and failure of coal body under different initial confining pressures are presented in Table 1.

3.1. RELATIONSHIP BETWEEN THE INITIAL CONFINING PRESSURE AND THE MECHANICAL PROPERTIES OF COAL BODY

Some representative data were selected to develop the total stress-strain curve of coal body, as shown in Figure 4.

Considering that the unloading point reflects the original rock environment under different buried depths, and the coal body is in the state of three-dimensional isobaric compaction, the unloading trend shown in Figure 4 indicates a good linear elastic change at the beginning. As shown in Figure 5, as the initial confining pressure increases, the failure strength, confining pressure and axial strain of coal body tend to increase accordingly, and the change of failure strength is particularly obvious, revealing a strong correlation. Meanwhile, according to Figure 5 the changes in the lateral strain and volumetric strain are not obvious, indicating that the high initial

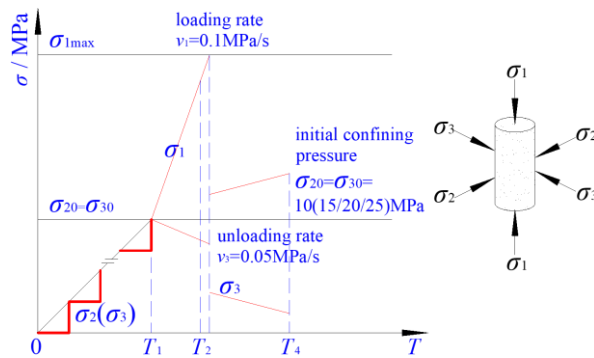


Fig. 3 The stress path of unloading confining pressure and loading axial pressure at different initial confining pressures.

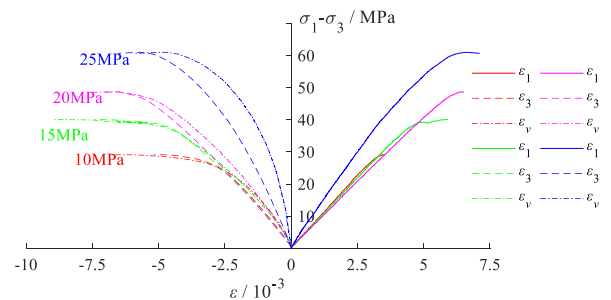
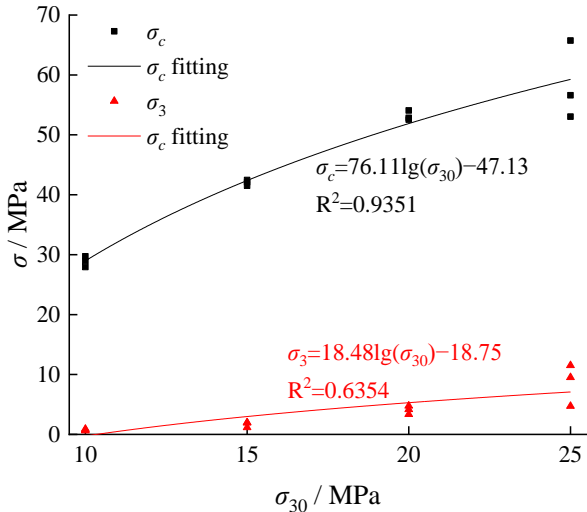
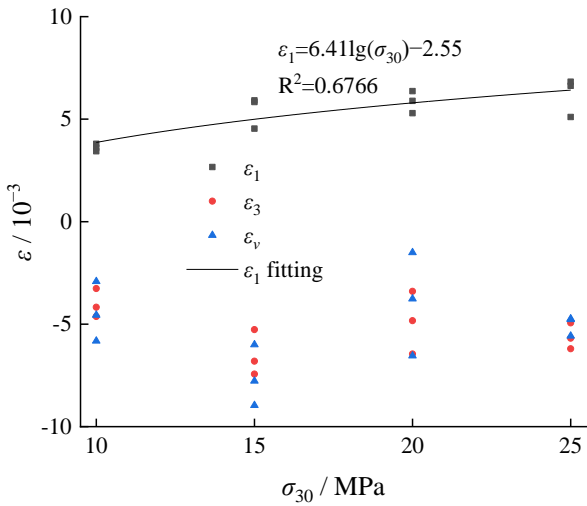


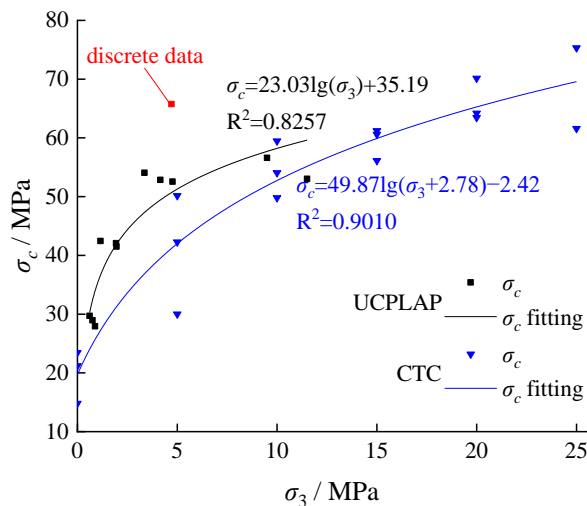
Fig. 4 The stress-strain curves.



(a) Failure strength and confining pressure



(b) Strain



UCPLAP-unloading confining pressure and loading axial pressure; CTC-conventional triaxial compression
(c) Failure strength-confining pressure

Fig. 5 The relationship among stress, strain and initial confining pressures.

confining pressure environment contributes to the prevention of the coal failure, resulting in a strengthening effect. Under the circumstance that the coal body is damaged, the failure strength shows a good nonlinear positive correlation with the confining pressure. Compared with the conventional triaxial compression strength, the failure strength of coal body under the corresponding confining pressure is significantly improved (as shown in Fig. 5c), which further indicates a strengthening effect due to the confining pressure, and some improvements to the failure strength of the coal body due to the unloading stress path.

As shown in Figure 6, with the increase of initial confining pressure, the time required to reach the failure increases nonlinearly. When the initial confining pressure is 25 MPa, the failure time is significantly different. In addition to the features of specimen itself, the higher initial confining pressure also causes various extents of damage to the coal body. With the unloading, the data of the failure time shows relatively obvious discreteness, which is confirmed by the failure strength under this condition shown in Figure 5a.

Combined with the logarithmic variation trend of each parameter in Figure 5 and Figure 6, the following conclusions can be drawn, including (1) the strengthening effect on coal body gradually weakens with the increase of initial confining pressure; (2) when the confining pressure exceeds a threshold value, the environment with a higher initial stress has led to the accumulation of the internal damage of coal body even close to failure. The unloading stress path provides an opportunity for the failure to occur. At this time, the failure strength and time-consuming of coal body remain basically unchanged, and the fluctuation in a certain range is mainly caused by the specimen itself.

At the failure, the relationship between the deformation parameters and the initial confining pressure is shown in Figure 7.

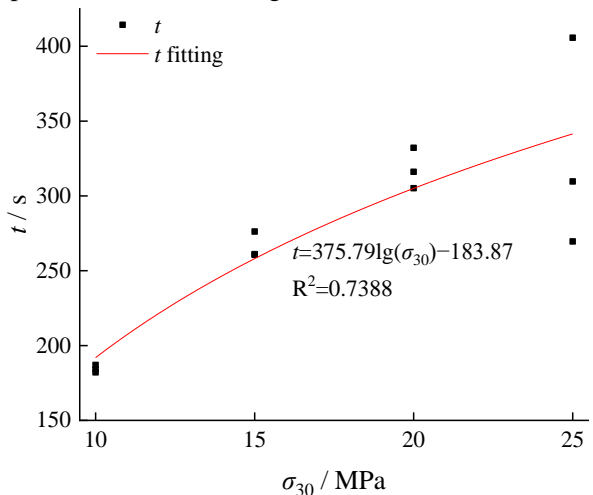
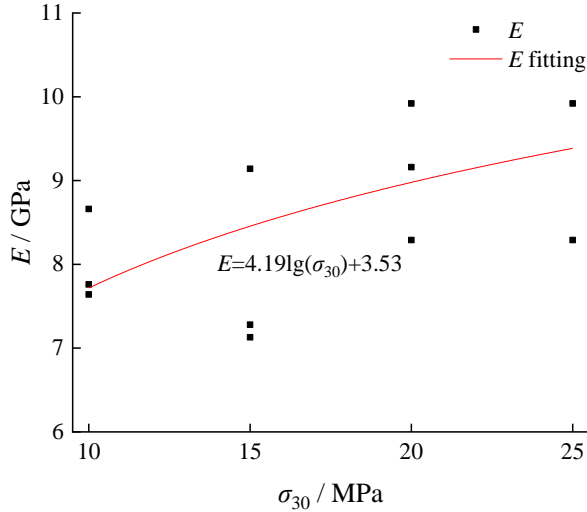
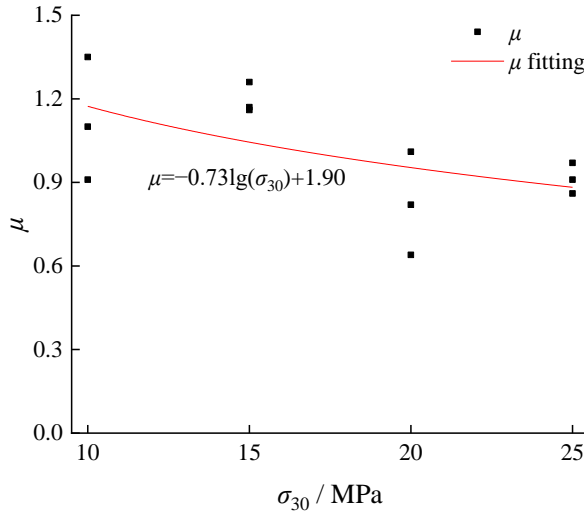


Fig. 6 Relationship between failure time and initial confining pressures.



(a) Elastic modulus



(b) Poisson's ratio

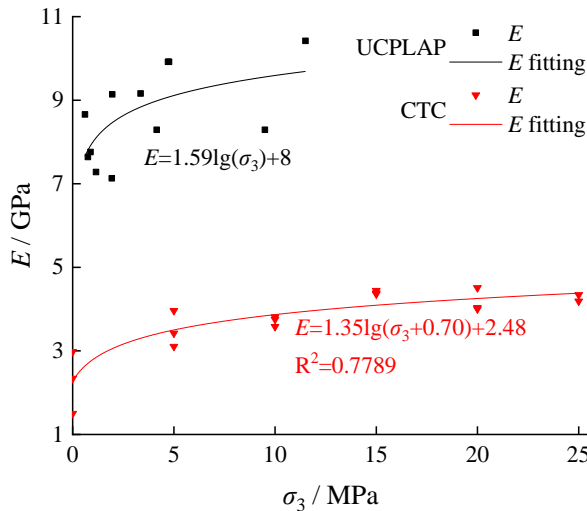

 UCPLAP-unloading confining pressure and loading axial pressure; CTC-conventional triaxial compression
 (c) Elastic modulus-confining pressure

Fig. 7 The relationship between deformation.

According to Figure 7, as the initial confining pressure increases, the elastic modulus at the time of coal failure increases nonlinearly as a whole, while the Poisson's ratio demonstrates an opposite trend with the overall downward trend, approaching to a stability. In this study, the development is not discussed as Poisson's ratios exceeds 0.6. The increase of the elastic modulus increases the deformation of coal body drastically with the enhanced brittleness characteristics. Compared with the elastic modulus under the conventional triaxial compression condition, it is also significantly improved (Fig. 7c), indicating that the unloading stress path is conducive to the brittle failure form development of coal body. Therefore, under the unloading state of high initial confining pressure, the coal body is more prone to brittle failure and the probability of inducing strong dynamic disasters will also increase significantly.

3.2. RELATIONSHIP BETWEEN INITIAL CONFINING PRESSURE AND ENERGY EVOLUTION OF COAL BODY

In the process of unloading confining pressure and loading axial pressure, it is assumed that the total input work U of the testing system consists of the positive work U_1 performed by axial pressure and the negative work U_3 performed by confining pressure, which is only transformed into elastic strain energy w_e and plastic strain energy w_d , the relationship can be expressed as

$$U = U_1 + U_3 = w_e + w_d, \quad (1)$$

whereas,

$$U_1 = \int_0^{\varepsilon_1(t)} \sigma_1 d\varepsilon_1, \quad U_3 = 2 \int_0^{\varepsilon_3(t)} \sigma_3 d\varepsilon_3,$$

$$w_e = \frac{1}{2} \sigma_1 \varepsilon_1.$$

Since the unloading point is the original rock state, a large amount of energy w_0 has been stored in the coal body, so Equation (1) can be rewritten as

$$U = w_0 + U_1 + U_3 = w_e + w_d. \quad (2)$$

Combined with the conventional triaxial compression experiment, the energy storage w_0 of coal body under different hydrostatic pressures is calculated following Equation (1), as shown in Figure 8.

The unloading experimental data and average energy storage under corresponding stress state are substituted into Equation (2) to obtain the energy evolution of coal body under different initial confining pressure, as shown in Figure 9.

As shown in Figures 9a-e, as the initial confining pressure increases, the positive work U_1 , total work U , elastic strain energy w_e , negative work U_3 and plastic strain energy w_d all show an increasing trend, and the regularity of the latter two is relatively poor, which is confirmed by the fitting result of all experimental data shown in Figure 9f. According to the logarithmic fitting relationship (as

shown in Fig. 9f), with the increase of initial confining pressure, the evolution of each strain energy gradually transforms into the calm stage from the intense stage. When the confining pressure exceeds a threshold value, the input energy before unloading reaches the limit of coal body bearing. Therefore, such changes can approximately reflect the energy changes in the state of high hydrostatic pressure. In addition, the strain energy difference is mainly caused by the specimen itself.

According to the relevant researches on rock burst, a greater volume of releasable elastic strain energy stored in coal and rock mass can often lead a higher probability of dynamic behaviors. Figure 10 shows the evolution process of elastic strain energy and the conversion rate at failure time of coal specimen under different initial confining pressures.

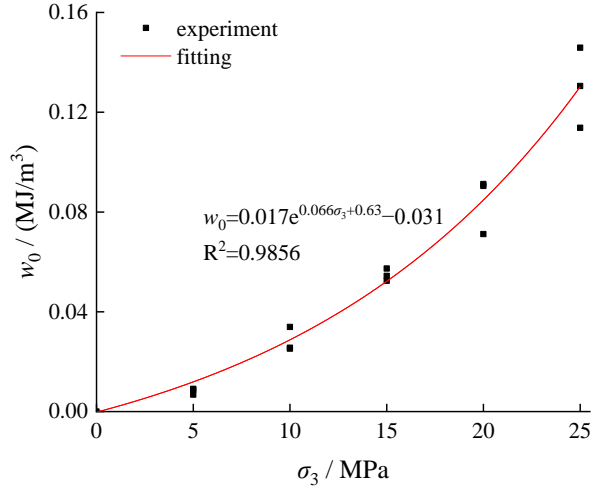
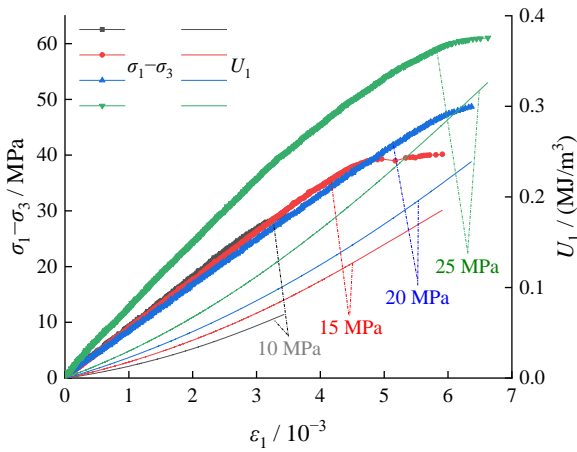
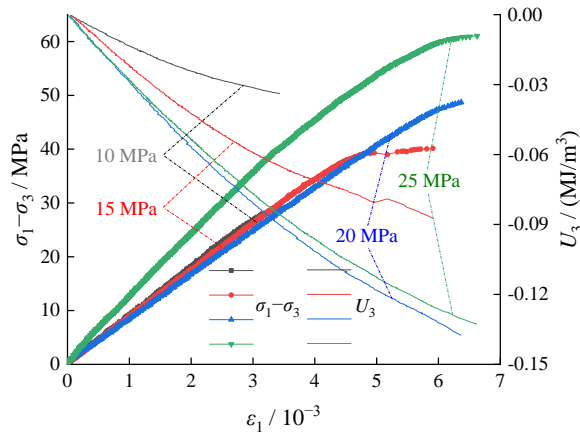


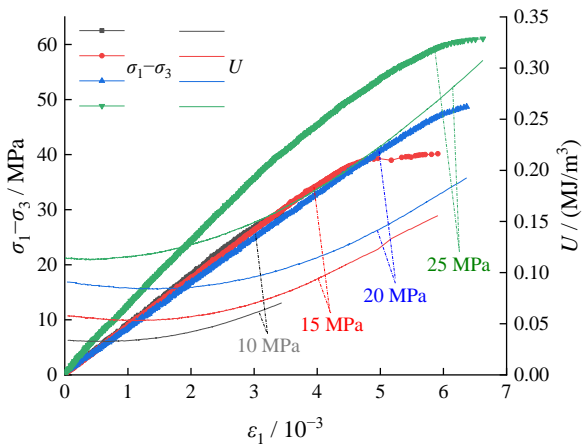
Fig. 8 Energy storage of coal body under different hydrostatic pressures.



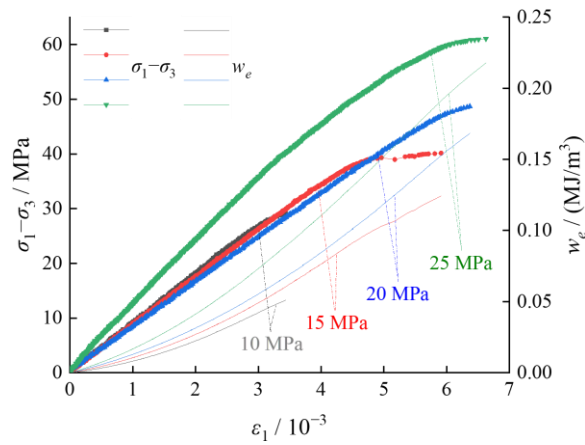
(a) The work of axial pressure U_1



(b) The work of confining pressure U_3



(c) The total work U



(d) The elastic strain energy w_e

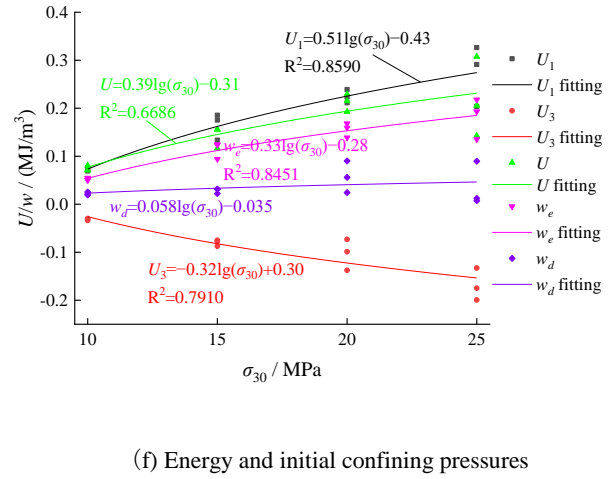
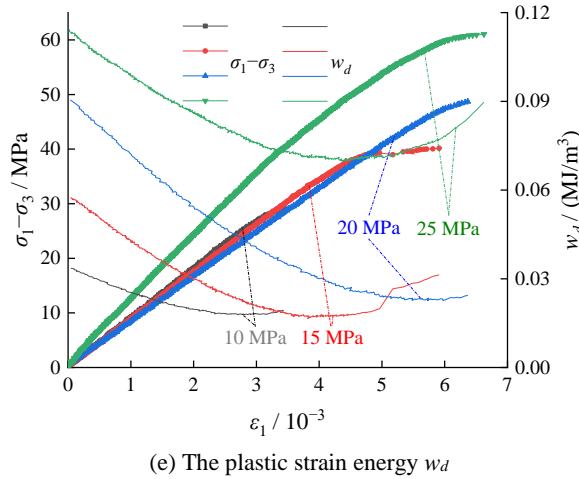
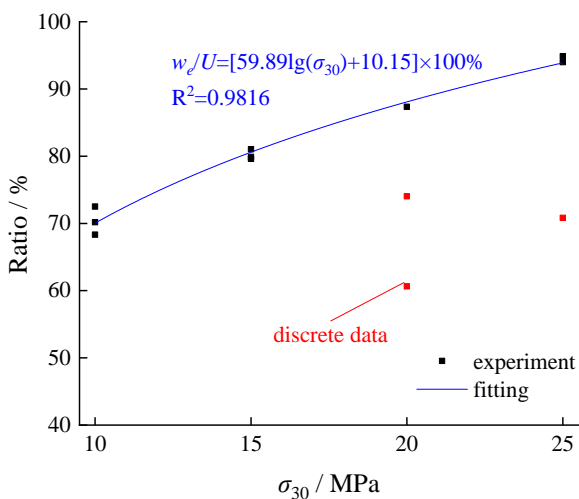
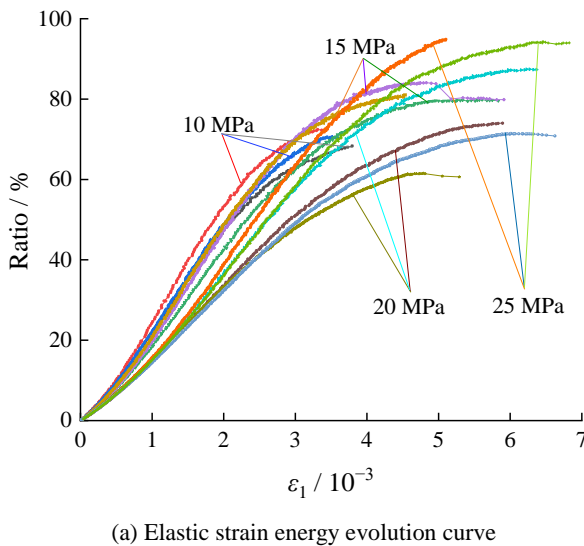


Fig. 9 Energy evolution curves.



(b) The conversion rate of elastic strain energy and initial confining pressures

Fig. 10 Elastic strain energy conversion ratios.

As shown in Figure 10a, the ratio of the input energy of the testing system to the elastic strain energy in the early stage of unloading (elastic state) increases approximately linearly, and then (plastic state) slowly increases to a fluctuating change. As shown in Figure 10b, the conversion rate of elastic strain energy increases nonlinearly with the increase of initial confining pressure at the time of coal failure. The high initial confining pressure increases the requirement of coal failure, and also increases the time required for unloading to failure. The input energy of the testing system increases and most of the energy is converted into elastic strain energy stored in the coal body. The brittle failure characteristics are obvious with sufficient energy to suddenly release, resulting in the increase of the risk and strength of dynamic failure, which is also one of the fundamental reasons for the difficulties in excavation support and maintenance, the strong ground pressure and the frequent occurrence of dynamic disasters in deep high stress mines.

3.3. DISCUSSION

For the original rock state coal body, the experimental unloading path and evolution process are different from the actual excavation unloading, and they are not completely the same, as shown in Figure 11.

In the actual excavation process, the studied coal body is restrained by the surrounding rock both axially and radially deep in the roadway. The unloading mainly occurs at the side of the free space of the roadway (as shown in Figure 11a), resulting in uneven confining pressure constraints in the circumferential direction. In the experiment, the studied coal body was unloaded as a whole in a circumferential direction (as shown in Figure 11b). Combined with the above research results, the following conclusions can be drawn: (1) under the same conditions (the initial confining pressure, the loading and unloading rate,

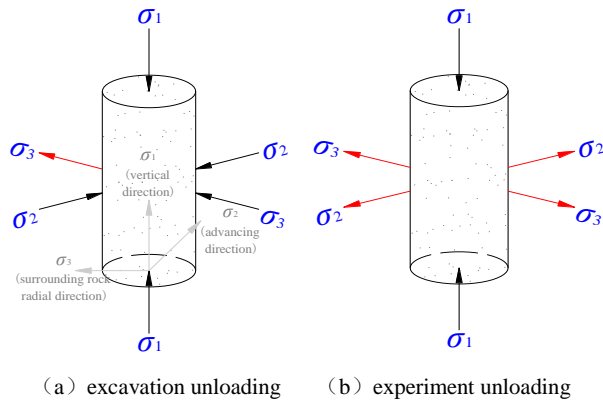


Fig. 11 Comparison of excavation unloading and experiment unloading.

and the time), the negative work done by the confining pressure to the surrounding rock (shallow) coal body of the actual excavation roadway is less than the work measured in the experimental coal body, indicating that more energy is expected to input into the former coal body. Therefore, the plastic strain energy dissipated by degradation or the stored elastic strain energy tends to be more sufficient. In the continuously deteriorating high-energy environment, the coal damage accumulates rapidly. Under the high storage elastic strain energy, the probability of dynamic disasters will increase significantly. In addition, the channels of pressure relief and energy release are mainly the free side of the roadway. In the event of an accident, the broken surrounding rock will be thrown to the roadway in a concentrated manner within a short period of time, resulting in highly destructive damage and hazards. (2) With the increase of initial confining pressure (burial depth), the natural energy storage of coal body rises exponentially, which significantly increases the risk of disaster induction. In order to ensure the construction safety, additional measures, such as mine pressure monitoring, joint pressure relief, support parameters and construction technology optimization, etc., have to be adopted in the actual production of deep mines (Zhao et al., 2021; Wang Q. et al., 2022; Sun et al., 2022).

The conclusions obtained from the research are in line with the actual production law, with some defects. For instance, (1) the stress state of the unloading point is not the actual or any three non-isobaric states, but a relatively ideal hydrostatic pressure state; (2) the specimens are not derived from the coal body under the condition of the corresponding burial depth of each initial confining pressure, which can impact the experiment to some degrees, especially in a simulated high-energy environment exceeding the actual burial depth. Regarding the decrease in the correlation of experimental data, in addition to the aforementioned factors, the specimen itself can be a source of influence on the accuracy of the experiment as well. In the future, the follow-up research of in-depth exploration is recommended to be conducted.

4. CONCLUSIONS

The stress path of unloading the confining pressure and loading the axial pressure conforms to the stress adjustment process of the surrounding rock in general excavation of underground engineering (such as roadway). Based on the experiment, the influence of the initial confining pressure on the mechanical properties and energy evolution law of coal body was analyzed, and the following conclusions were obtained:

1. As the initial confining pressure increases, the peak strength, the confining pressure and the axial strain increase nonlinearly at the coal failure, with enhanced brittle failure characteristics, while the variation law of the lateral strain and the volumetric strain is not obvious. Compared with the conventional triaxial compression experiment, the unloading stress path can strengthen the failure strength and brittle failure characteristics of coal body to a certain extent.
2. As the initial confining pressure increases, the natural energy storage of coal body increases sharply in exponential form. During the unloading, the positive work performed by the axial pressure, the negative work performed by the confining pressure, the total work, the elastic strain energy and the plastic strain energy all increase nonlinearly. In addition, the energy evolution inside the coal body changes from the intense stage to the calm stage, with the conversion rate of elastic strain energy increasing nonlinearly, resulting in a higher risk and intensity of dynamic failures.
3. It is worth pointing out that some differences have been identified between the stress adjustment of surrounding rock in actual excavation and the unloading of pseudo-triaxial experiment. With the increase of initial confining pressure (buried depth), the risk of disaster induced by actual construction environment increases significantly. Joint pressure relief measures are currently one of the effective methods to ensure the safe and efficient production in deep mines.

DATA AVAILABILITY

The data used to support the findings of the study are available from the corresponding author upon request.

CONFLICTS OF INTEREST

The authors declare that no conflict regarding the publication of this paper has been identified.

ACKNOWLEDGMENTS

This study was supported by the National Natural Science Foundation of China Youth Project (52404122), the Jiangsu University "Blue Project" Funding, the Chongqing PhD Express Project (CSTB2023NSCQ-BSX0009), the Jiangsu Province

Industry University Research Cooperation Project (BY2021188). We thank Xuzhou Yu-Yi (Science and Technology Consulting Service Co., Ltd.) for editing the English text of the draft of this manuscript.

REFERENCES

- Chen, X., Li, L. and Qi, L.: 2019, The current situation and prevention and control countermeasures for typical dynamic disasters in kilometer-deep mines in China. *Safety Sci.*, 115, 229–236. DOI: 10.1016/j.ssci.2019.02.010
- Cui, F., Zhang, T., Lai, X., Wang, S., Chen, J. and Qian, D.: 2021, Mining disturbance characteristics and productivity of rock burst mines under different mining intensities. *J. China Coal Soc.*, 46, 12, 3781–3793, (in Chinese).
- Guo, H., Ji, M., Liu, D., Liu, M., Li, G. and Chen, J.: 2021, An experimental research on surrounding rock unloading during solid coal roadway excavation. *Geofluids*, 2021, 1–9. DOI: 10.1155/2021/5604642
- Guo, H., Sun, Z., Ji, M., Liu, D., Wu, Y. and Nian, L.: 2022a, A study on the effects of loading axial pressure rate on coal mechanical properties and energy evolution law. *Geofluids*, 2022, 1–11. DOI: 10.1155/2022/5593173
- Guo, H., Sun, Z., Ji, M., Wu, Y. and Nian, L.: 2022b, An investigation on the impact of unloading rate on coal mechanical properties and energy evolution law. *Int. J. Environ. Res. Public Health*, 19, 8, 4546. DOI: 10.3390/ijerph19084546
- He, M.: 2021, Research progress of deep shaft construction mechanics. *J. China Coal Soc.*, 46, 3, 726–746, (in Chinese).
- Huang, B., Zhang, N., Jing, H., Kan, J., Meng, B., Li, N., Xie, W. and Jiao, J.: 2020, Large deformation theory of rheology and structural instability of the surrounding rock in deep mining roadway. *J. China Coal Soc.*, 45, 3, 911–926, (in Chinese).
- Kang, H., Wang, G., Jiang, P., Wang, J., Zhang, N., Jing, H., Huang, B., Yang, B., Guan, X. and Wang, Z.: 2018, Conception for strata control and intelligent mining technology in deep coal mines with depth more than 1000 m. *J. China Coal Soc.*, 43, 7, 1789–1800, (in Chinese). DOI: 10.1016/j.egy.2022.02.093
- Sun, Y., Bi, R., Sun, J., Zhang, J., Taherdangkoo, R., Huang, J. and Li, G.: 2022, Stability of roadway along hard roof goaf by stress relief technique in deep mines: a theoretical, numerical and field study. *Geomech. Geophys. Geo-Energy Geo-Res.*, 8, 2, 45. DOI: 10.1007/s40948-022-00356-8
- Wang, Q., Wang, Y., He, M., Li, S., Jiang, Z., Jiang, B., Xu, S. and Wei, H.: 2022, Experimental study on the mechanism of pressure releasing control in deep coal mine roadways located in faulted zone. *Geomech. Geophys. Geo-Energy Geo-Res.*, 8, 2, 50. DOI: 10.1007/s40948-021-00337-3
- Wang, X., Zhang, H., Chen, Q., Zeng, Q. and Liu, J.: 2022, Acoustic emission characteristics and damage model of limestone loading with different rockburst tendencies. *Chin. J. Rock Mech. Eng.*, 41, 7, 1373–1383, (in Chinese).
- Wu, F., Zhang, H., Zou, Q., Li, C. and Cao, Z.: 2022, In-situ stress distribution laws of coal and rock in deep mining based on the Griffith criterion. *Geomech. Geophys. Geo-Energy Geo-Res.*, 8, 2, 78. DOI: 10.1007/s40948-022-00395-1
- Xie, H.: 2019, Research review of the state key research development program of China: deep rock mechanics and mining theory. *J. China Coal Soc.*, 44, 5, 1283–1305, (in Chinese).
- Xie, H., Gao, F., Ju, Y., Gao, M., Zhang, R., Gao, Y., Liu, J. and Xie, L.: 2015, Quantitative definition and investigation of deep mining. *J. China Coal Soc.*, 40, 1, 1–10, (in Chinese).
- Xie, H., Gao, M., Zhang, R., Peng, G., Wang, W. and Li, A.: 2019, Study on the mechanical properties and mechanical response of coal mining at 1000 m or deeper. *Rock Mech. Rock Eng.*, 52, 5(SI), 1475–1490. DOI: 10.1007/s00603-018-1509-y
- Yan, X., Guo, C., Liu, Z., Wang, Y., Liu, D. and Liu, G.: 2022, Physical simulation experiment of granite rockburst in a deep-buried tunnel in kangding county, Sichuan province, China. *Earth Sci.*, 47, 6, 2081–2093, (in Chinese).
- Yang, Y., Ai, T., Zhang, Z., Zhang, R., Ren, L., Xie, J. and Zhang, Z.: 2020, Acoustic emission characteristics of coal samples under different stress paths corresponding to different mining layouts. *Energies*, 13, 12, 3295. DOI: 10.3390/en13123295
- Yuan, L.: 2021, Research progress of mining response and disaster prevention and control in deep coal mines. *J. China Coal Soc.*, 46, 3, 716–725, (in Chinese).
- Zeng, Q., Huang, X., Wang, X., Chen, Q., Liu, J. and Gong, C.: 2021, Experimental study on rock burst tendency and acoustic emission characteristics of limestone at different buried depths. *Gold Sci. Tech.*, 29, 6, 863–873, (in Chinese).
- Zhang, H., Fan, J., Guo, J., Shi, X. and Sun, F.: 2022, Rockburst tendency for deep underground engineering based on multi-parameters criterion. *Chin. J. High Press. Phys.*, 36, 2, 176–189, (in Chinese).
- Zhao, X., Zhou, X., Zhao, Y. and Yu, W.: 2021, Research status and progress of prevention and control of mining disasters in deep metal mines. *J. Cent. South Univ. (Sci. and Tech.)*, 52, 8, 2522–2538, (in Chinese).
- Zhao, Y.: 2021, Retrospection on the development of rock mass mechanics and the summary of some unsolved centennial problems. *Chin. J. Rock Mech. Eng.*, 40, 7, 1297–1336, (in Chinese).
- Zhou, J., Zhang, J., Wang, J., Li, F. and Zhou, Y.: 2022, Research on nonlinear damage hardening creep model of soft surrounding rock under the stress of deep coal resources mining. *Energy Rep.*, 8, S4, 1493–1507.